Analyzing Power Studies for Longitudinal Polarimeter

Justin Schnettler and Wolfgang Lorenzon

April 19, 2001

Abstract

GEANT Monte Carlo simulations have been performed to study the dependence of the analyzing power measured with the $NaBi(WO_4)_2$ calorimeter on the amount of material in front of the photomultiplier tubes. The simulations confirm the experimentally observed 25% increase in the analyzing power and demonstrate why the analyzing power did not change when the 17-cm long $NaBi(WO_4)_2$ crystals were exchanged with 20-cm long crystals (present setup). The analyzing power A_0 measured in the photomultiplier tubes was simulated using a Compton generator and realistic beam smearing parameters.

Contents

1 Introduction

This report summarizes the GEANT MC simulations that can explain the 25% effect that was measured with the longitudinal polarimeter when the nickel foil was insterted in the $NaBi(WO_4)_2$ calorimeter. [1]

A large number of Compton photons can be produced per laser pulse when the polarimeter is operated in the multi-photon mode, ranging from a few photons to many thousand. During normal operating mode in which about 600 back-scattered Compton photons are produced at the beginning of a fill, approximately 150 times more energy is deposited in the calorimeter than the highest energies (bremsstrahlung) deposited in the single-photon mode, since the average energy deposited per Compton photon is 6.8 GeV. In order to attenuate the Čerenkov light to protect the photomultiplier tubes from saturation, a remotely controlled movable, perforated nickel foil could be inserted into the 3 mm air gap between the $NaBi(WO_4)_2$ crystals and the photomultiplier tubes. This used to be the standard mode of operation for the longitudinal polarimeter, and is displayed in Fig. 1a.

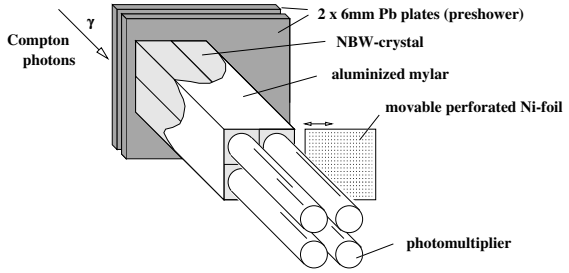

Figure 1a) Schematic layout of the original $NaBi(WO_4)_2$ calorimeter. During systematic studies, either a nickel foil, a neutral density filter or no light absorber was insterted between the four $NaBi(WO_4)_2$ crystals and the four photomultiplier tubes.

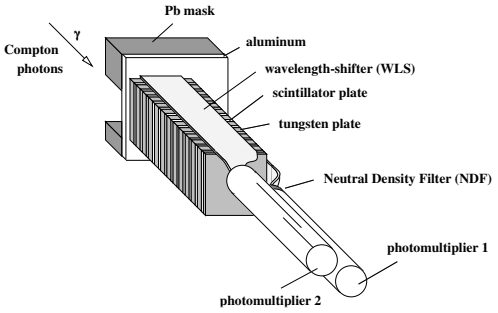

Figure 1b) Schematic layout of the prototype sampling calorimeter [2]. It was designed to do multi-photon operation with a neutral density filter before photomultiplier 1 and single-photon operation with no absorber before photomultiplier 2.

Even though the $NaBi(WO_4)_2$ crystals are 19 radiation lengths long, there is a small amount of longitudinal shower leakage into the photomultiplier tubes. Unfortunately, the corresponding shower particles can generate a large signal in the photomultiplier tubes which subsequently can introduce a substantial non-linearity in the energy response. The longitudinal shower leakage signal derives mostly from the highest energy Compton photons and hence has a large analyzing power (A_{leak}). Therefore, the photomultiplier signal has two components (neglecting indirect light from wall reflections, etc.) that contribute to the total analyzing power (A_{tot}) which is given by

$$A_{tot} = f_{NBW} \cdot A_{NBW} + f_{leak} \cdot A_{leak}, \tag{1}$$

where f_{NBW} and f_{leak} are the relative contributions to the total analyzing power due to the light produced in the $NaBi(WO_4)_2$ crystals and the longitudinal shower leakage, respectively, and $A_{NBW} = 0.1838$ is the nominal analyzing power, based on the polarized Compton cross section. As shown in Fig. 1a), various filters (nickel foil or neutral density filters) with optical attenuation att_{opt} could be used to attenuate the Čerenkov light from the $NaBi(WO_4)_2$ crystals into the photomultiplier tubes. When optical filters are used, Eq. 1 needs to be modified slightly by replacing f_{NBW} by $\frac{f'_{NBW}}{att_{opt}}$ such that the normalization condition $\frac{f'_{NBW}}{att_{opt}} + f_{leak} = 1$ is fulfilled. Therefore, as the Čerenkov light produced in the $NaBi(WO_4)_2$ crystals was attenuated by the optical filters, the

shower leakage signal started to dominate the signal in the photomultiplier tubes. In the case of using the nickel foil, this altered the response function and increased the analyzing power of the detector by about 25 %.

In order to be able to better study the source of this 25 % deviation, a second calorimeter was built with much better energy resolution. The prototype sampling calorimeter, as shown in Fig. 1b, was constructed such that it could be operated both in single-photon and multi-photon mode. The advantages of the single-photon mode were that the asymmetries are large, up to 0.60 at the Compton edge, and that the energy spectra could be compared to the Compton cross sections. However, single-photon mode is not a feasible mode of operation with the 100 Hz laser, since a measurement of the beam polarization with an absolute statistical accuracy of 0.01 takes about 2.5 hours. In comparison, such a measurement takes only one minute in the multi-photon mode.

The prototype sampling calorimeter is discussed here only for the sake of comparing testbeam results with the MC simulations. It was never used to provide polarization data to Hermes. Based on the results obtained from the prototype sampling calorimeter, Carol Scarlett developed a new and improved sampling calorimeter [3], which is modelled in the MC simulations discussed in this report.

2 Setup

The sampling calorimeter configuration used in some of the MC simulations is shown in Fig. 2. Here, the sampling calorimeter is shown toghether with a single photomultiplier tube, which is located 80 mm behind the detector. The window of the photomultiplier tube was modelled as a quartz glass cylinder of 17 mm diameter and 3 mm thickness. In the simulation of the sampling calorimeter configuration, we used 24 scintillator plates (40 mm $\times$ 40 mm $\times$ 2.6 mm) and 25 densimet plates (40 mm $\times$ 40 mm $\times$ 3.0 mm), yielding a total tickness of 18.3 X_0 (0.15+18.15 X_0). The calorimeter enclosure was made of 10 mm thick aluminum plates.

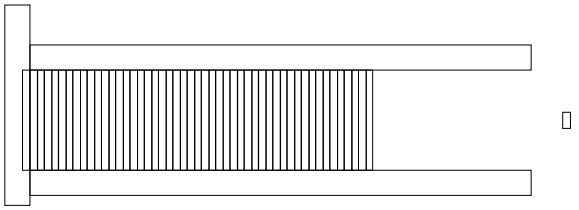

Figure 2. Schematic layout of GEANT MC geometry for the sampling calorimeter. The photomultiplier tube was always located 8 cm behind the detector material, independent of the detector thickness.

It is not pratical to track individual Čerenkov or scintillation photons in the GEANT MC code. Therefore, it was not possible to extract f_{NBW} and f_{leak} from the MC, and we restricted ourselves to compute A_{leak}. For most of the MC simulations, the sampling detector was therefore replaced by a pure densimet block, varying in thickness between 1.2 X_0 and 27.8 X_0 to speed up the simulation by about a factor of four. This was based on the assumption, that the longitudinal shower leakage into the photomultiplier tubes does not depend on the specific material, but rather on the amount of material in terms of radiation length (X_0). We have explicitly tested this assumption by comparing the analyzing power for a pure denismet detector and for the sampling calorimeter, as shown in Table 1.

Instead of tracking individual photons, we made a simple model. We assumed (see Eq. 1) that the main source of light in the photomultiplier tubes, besides the light from the detector (f_{NBW}),

comes from Čerenkov light produced in the photomultiplier tube glass windows (f_{leak}).[1] We further assumed that the signal in the photomultiplier tubes could be either proportional to the number of electrons or positrons hitting the photomultiplier tube windows, or to the energy deposited by electrons or positrons in the photomultiplier tube glass window.

3 Simulation of Analyzing Power

The simulations were carried out using two different models for creating a signal in the photomultiplier tubes. First of all, the primary light, or the light produced in the detector, was not allowed to enter the photomultiplier tube, by setting $f_{NBW} = 0$. This was done to compare to the experimental situation where the photomultiplier tubes in the calorimeter were covered with black tape to prevent any primary light from reaching the photomultiplier tubes. Therefore, only secondary "light", resulting from interactions with charged particles in the photomultiplier tube windows or photocathodes was investigated ($f_{leak} = 1$). Here we assumed that the secondary light could have been produced by Čerenkov light in the glass of the photomultiplier tube, by either counting all the charged particles (electrons or positrons) that entered the photomultiplier tube, or by measuring the total energy deposited by all the charged particles that had interactions in the glass of the photomultiplier tube.

The first model – just counting electrons or positrons hitting the photomultiplier glass window – was set up by putting the following conditions in the GEANT subrotine 'gustep.f':

```
*
*     ask for particles (electrons or positrons) that enter a new volume
*     called (PMT1) which is a detector
*
      IF((IPART.EQ.2 .OR. IPART.EQ.3) .AND. INWVOL.EQ.1
          .AND. NAMES(NLEVEL).eq.'PMT1' .AND. ISVOL.NE.0) THEN
*
```

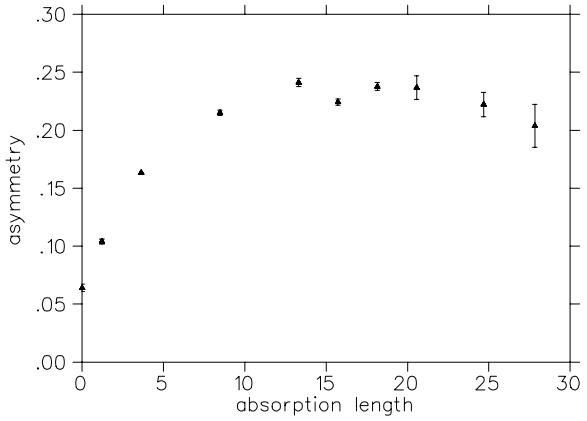

Figure 3.a Uncorrected asymmetry in the number of charged particles passing through the photomultiplier as a function of detector material in radiation lengths before the photomultiplier.

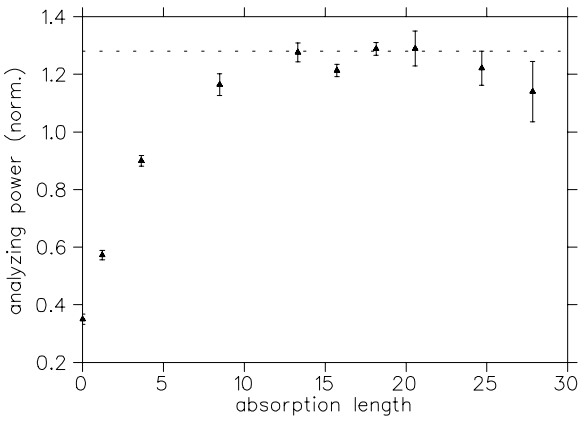

Figure 3.b Analyzing power in the number of charged particles passing through the photomultiplier as a function of detector material in radiation lengths before the photomultiplier. The dashed line indicates the values measured for the NBW calorimeter.

[1] photomultiplier tube glass is usually not a very good scintillator material.

The results from the first model are presented in Figs. 3.a and 3.b. Fig. 3.a shows that the asymmetry in the number of charged particles hitting the photomultiplier glass window increases from about 6% [2] for a zero radiation length (X_0) configuration to about 23.5% for a detector that is between 13 X_0 to 21 X_0 long. Note that the expected asymmetry is 18.4%. It is expected that the asymmetry measured in the photomultiplier is larger than the physics asymmetry of the Compton process because the longitudinal shower leakage signal derives mostly from the highest energy Compton photons which have a large analyzing power. As more detector material is added, the number of particles penetrating the rear end of the detector decreases rapidly and the asymmetry starts to drop again. Fig. 3.b shows the simulated data again, but now each point is normalized to the analyzing power obtained from the MC, which fluctuates within statistics from the nominal value of 18.4% for each simulation. The dashed line ($A = 1.28$) indicates the values measured for the NBW calorimeter.

The second model, as displayed in Fig. 4 – recording the total energy deposited by all electrons or positrons hitting the photomultiplier glass window – was set up by putting the following conditions in the GEANT subrotine 'gustep.f':

```
*
*     ask for particles (electrons or positrons) found in the volume called
*     (PMT1) which is a detector
*
      IF((IPART.EQ.2 .OR. IPART.EQ.3) .AND. NAMES(NLEVEL).eq.'PMT1'
          .AND. ISVOL.NE.0) THEN
*
```

The results from the second model are presented in Figs. 4.a and 4.b. They show the exact same behaviour as the data presented in Figs. 3.a and 3.b.

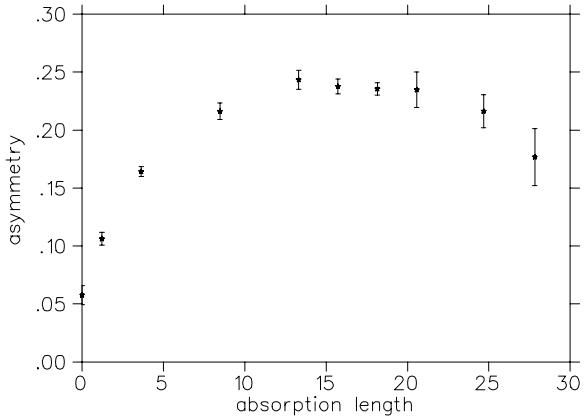

Figure 4.a Uncorrected asymmetry in the total energy deposited by all charged particles passing through the photomultiplier as a function of detector material in radiation lengths before the photomultiplier.

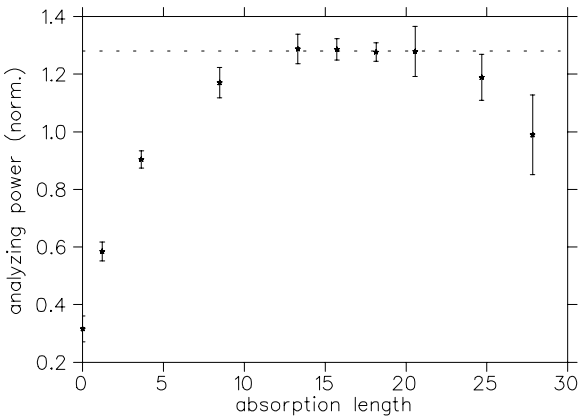

Figure 4.b Analyzing power in the total energy deposited by all charged particles passing through the photomultiplier as a function of detector material in radiation lengths before the photomultiplier. The dashed line indicates the values measured for the NBW calorimeter.

[2] Note, that the cross section asymmetry for a 2.33 eV photon scattered off a 27.5 GeV electron is 6.12%.

Table 1: Comparison of analyzing power for a sampling calorimeter (25 plates) and a pure densimet calorimter (7.5 cm), both of which have 18.15 X_0. The radiation length for densimet is 0.413 cm.

Model	Densimet	Sampling Calorimeter
1 (hits only)	1.289 ± 0.022	1.305 ± 0.029
2 (energy deposited)	1.280 ± 0.038	1.291 ± 0.020

4 Comparison with Measurements

The simulations have been compared with the values measured for the $NaBi(WO_4)_2$ crystal and the prototype sampling calorimeter configurations, which are presented in Tables 2 and 3, respectively [4]. The standard running configuration for all of 1996, 1997, and up until July 1998, was the $NaBi(WO_4)_2$ crystal with the nickel foil inserted. The ratio of the beam polarization measured between the longitudinal and transverse polarimeters (LPOL/TPOL) was 1.28, and was loosely called"the 25% effect". As it can be seen both in Figs. 3.b and 4.b, this ratio is very well reproduced by the GEANT MC program in the 13 to 21 X_0 region. Configuration (3) in Table 2 is not consistent with the expected ratio of 1.0, because the relative response function of the $NaBi(WO_4)_2$ calorimeter was found to be non-linear, as shown in Fig. 5.

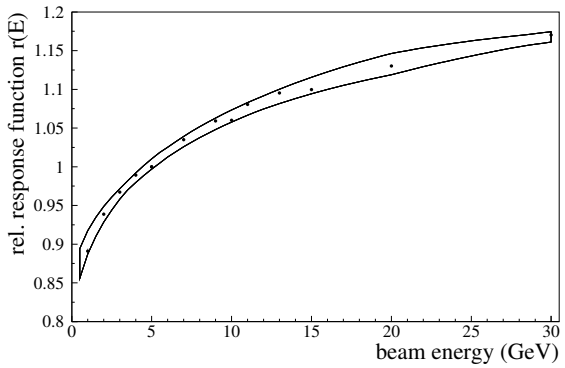

Figure 5. Relative $NaBi(WO_4)_2$ calorimeter response function, normalized to unity at 5 GeV, as determined in the DESY T22 and CERN X5 test beams. The band represents the systematic uncertainty.

That non-linear behaviour is of course expected because the longitudinal shower leakage increases with higher Compton photon energy for a fixed calorimeter configuration. After accounting for this non-linearity, the ratio (LPOL/TPOL) is $1.026 \pm 0.010(\text{stat}) \pm 0.009(\text{analyzing power})$. Since July 1998, the $NaBi(WO_4)_2$ crystal calorimeter has been operated without optical attenuators and is now a standolne calorimeter, e.g. there is neither a calibration with respect to the transverse polarimeter nor a rise-time calibration necessary anymore.

Table 2: Test of specific light attenuation configurations for NBW crystal calorimter.

	Configuration	opt. atten.	ratio (LPOL/TPOL)
(1)	NBW + Ni-foil	80	1.28 ± 0.01
(2)	NBW + NDFilter	10	1.14 ± 0.01
(3)	NBW + no attenuation	1	1.08 ± 0.01
(3')	NBW corrected for non-linearity	1	$1.026 \pm 0.010 \pm 0.009$

A cross check with the prototype sampling calorimeter also showed very similar results. There

was some slight discrepancy between photomultiplier 1 and 2 for configurations (3) and (4), respectively, which has not yet been accounted for. In addition, Table 2 suggests, that f_{leak} is approximately 0.1%. However, the model desribed in Eq.1 holds only marginally in the case of the $NaBi(WO_4)_2$ calorimeter, and it is estimated by Ref. [4] that f_{leak} is about 10%. Please note that this is not a problem for comparing the MC results with the measurements, because operating the calorimeter with a nickel foil ($att_{opt} = 80$) introduces only a small contimination (0.011 if $f'_{NBW} = 90\%$) to the extraction of A_{tot} in Eq. 1. This is consistent with the statistical uncertainties of the MC simulations.

Table 3: Test of specific light attenuation configurations for prototype sampling calorimeter.

	Configuration	opt. atten.	ratio (LPOL/TPOL)
(1)	PMT1 + NDF	10^4	1.30 ± 0.01
(2)	PMT2 + NDF	10^4	1.30 ± 0.03
(3)	PMT1	1	1.00 ± 0.01
(4)	PMT2	1	1.045 ± 0.01

5 Conclusions

Detailed GEANT MC simulations have been performed which reproduce the "25% effect" that plagued the longitudinal polarimeter since it started data taking in 1996. The simulations confirm the preliminary MC studies done in August 1999 [3], which lead to a series of measurements with the prototype sampling calorimeter. These simulations and subsequent tests were cruicial for a complete understanding of the physical processes occurring in the calorimeter and for the design of the new sampling calorimeter [3]. It showed the necessity that $f_{NBW} >> f_{leak}$ was absolutely essential to prevent large deviations in the analyzing power of the calorimeter.

The simulations also confirmed our observations that the analyzing power of the calorimeter did not change when we exchanged the 17-cm (16.5 X_0) long $NaBi(WO_4)_2$[5] crystals with 20-cm (19.4 X_0) long crystals in July 1998 (just before the CERN test beam measurements).

References

[1] M. Beckmann at al., Nucl. Instr. Meth. **AXXX**, in print

[2] The prototype sampling calorimeter was built by Joachim Seibert of the University of Freiburg.

[3] Carol Scarlett and Wolfgang Lorenzon, "A new sampling calorimeter for the longitudinal polarimeter at Hermes", Internal Polarimeter Report IPR-00-3, (Oct 2000),

[4] DESY-PRC Closed Session presentation by Armand Simon for the Polarization 2000 project on November 19, 1999. Co-authors of the report are J. Franz, F. Menden, C. Schill, and A. Simon, all of the University of Freiburg.

[5] The radiation length for $NaBi(WO_4)_2$ is 1.032 cm.

[3] The preliminary MC simulations were presented at DESY on Aug 20, 1999

A GEANT Monte Carlo Simulation Results

We present here the results obtained from the GEANT Monte Carlo simulations, which were used to extract the data shown in Figs. 3 and 4. The columns provide the filenames (which for e.g. line 1a include the number of events simualted (370,000), the thickness of the tungsten plate (11.5 cm), the MC generated analyzing power A_0, and the statistical error dA_0, the asymmetry in the total energy deposited by all electrons or positrons hitting the photomultiplier glass window E_0 and its statistical error dE_0, and the number of hits for the parallel (anti-parallel) spin configurations hits[+] (hits[-]). Note that there are two rows for each detector thickness. The filenames for the rows labeled with "a" ("b") represent the results if model 2 (model 1) was employed. Also note that model 1 does not provide any information about the total energy deposited in the photomultiplier glass window.

	filename	W(cm)	A_0	dA_0	E_0	dE_0	hits[+]	hits[-]
1a	leak-370k-p11.5-ene.hbk	11.5	0.1787	0.0019	0.1768	0.0246	9376	6515
1b	leak-370k-p11.5.hbk	11.5	0.1787	0.0019	0.0	0.0	1663	1100
2a	leak-390k-p10.2-ene.hbk	10.2	0.1820	0.0018	0.2164	0.0143	28341	18172
2b	leak-390k-p10.2.hbk	10.2	0.1820	0.0018	0.0	0.0	5199	3308
3a	leak-100k-p8.5-ene.hbk	8.5	0.1836	0.0036	0.2348	0.0152	28559	18279
3b	leak-100k-p8.5.hbk	8.5	0.1836	0.0036	0.0	0.0	5721	3531
4a	leak-380k-p7.5-ene.hbk	7.5	0.1845	0.0018	0.2356	0.0054	229390	142798
4b	leak-380k-p7.5.hbk	7.5	0.1845	0.0018	0.0	0.0	49391	30416
5a	leak-250k-p6.5-ene.hbk	6.5	0.1848	0.0023	0.2377	0.0063	313048	199895
5b	leak-250k-p6.5.hbk	6.5	0.1848	0.0023	0.0	0.0	73551	46603
6a	leak-69k-p5.5-ene.hbk	5.5	0.189	0.004	0.2434	0.0082	180877	112607
6b	leak-69k-p5.5.hbk	5.5	0.189	0.004	0.0	0.0	45984	28109
7a	leak-42k-p3.5-ene.hbk	3.5	0.1847	0.0056	0.2162	0.0072	352526	231115
7b	leak-42k-p3.5.hbk	3.5	0.1847	0.0056	0.0	0.0	111090	71771
8a	leak-100k-p1.5-ene.hbk	1.5	0.1816	0.0036	0.1642	0.0043	1006250	729345
8b	leak-100k-p1.5.hbk	1.5	0.1816	0.0036	0.0	0.0	415962	299114
9a	leak-100k-p0.5-ene.hbk	0.5	0.1817	0.0036	0.1063	0.0056	300482	244446
9b	leak-100k-p0.5.hbk	0.5	0.1817	0.0036	0.0	0.0	128629	104377
10a	leak-500k-p0.0-ene.hbk	0.0	0.1829	0.0016	0.0578	0.0082	112388	98530
10b	leak-500k-p0.0.hbk	0.0	0.1829	0.0016	0.0	0.0	50436	44372